ECCOMAS Congress 2016
VII European Congress on Computational Methods in Applied Sciences and Engineering
M. Papadrakakis, V. Papadopoulos, G. Stefanou, V. Plevris (eds.)
Crete Island, Greece, 5–10 June 2016

THE ROLE OF THE PRESTRESSED TENDONS ON THE SEISMIC PERFORMANCE OF HYBRID ROCKING BRIDGE BENTS

Anastasios I. Giouvanidis[1], **Elias G. Dimitrakopoulos**[2]

[1]Department of Civil and Environmental Engineering, The Hong Kong University of Science and Technology
Kowloon Bay, Hong Kong
e-mail: agiouvanidis@connect.ust.hk

[2] Department of Civil and Environmental Engineering, The Hong Kong University of Science and Technology
Kowloon Bay, Hong Kong
e-mail: ilias@ust.hk

Keywords: rocking bridges, flag-shaped hysteretic behavior, self-centering, prestressed tendons.

Abstract. *Allowing structural members to uplift and rotate around pre-defined pivot points isolates and relieves the structure from deformation and damage during strong earthquakes. Such rocking behavior has been examined as damage avoidance seismic design for bridges. Rocking structures, either freestanding or hybrid (supplemented with energy dissipation and re-centering devices), have been proposed by several researchers as high-performance systems that can survive major earthquakes without substantial damage. This paper investigates, analytically and numerically, the seismic performance of a hybrid rocking bridge bent which exhibits flag-shaped hysteretic behavior. The rocking frame is enhanced with elastic prestressed central tendons to provide re-centering capacity and hysteretic buckling restrained braces to dissipate energy. The present study examines its seismic behavior under both pulse-type and non-pulse-type ground motions. The focus of the present analysis is on the role of the prestressing force on the seismic performance. The results reveal the diverse influence of prestress. Specifically, prestress is beneficial for small rocking rotations, but could become detrimental when the frame sustains large rotations and as the size of the columns increases. Finally, the results reveal the sensitivity of the different rocking design solutions to the characteristics of the considered ground motion. As a consequence, none of the examined rocking frames can be considered as the optimal design solution under all ground motions.*

1 INTRODUCTION

Rocking as a means of seismic isolation is attracting the interest of researchers for almost a century (see [18, 16, 29, 6, 13, 9, 10, 30, 8, 39, 34] and references therein). Recently, there is an increasing need to examine the dynamics of progressively more complicated and realistic structures ([1, 2, 40, 38] among others). Of particular interest for bridge engineering is the rocking frame configuration of Fig. 1 proposed originally by [22] as a "damage avoidance design" for bridges. The existing bridges designed to rock remain scarce (see [11] and references therein), even though, an increasing number of studies illustrate their high seismic performance. In particular, [7, 33, 35, 36] revealed that rocking piers can exhibit large drifts (around 6% to 10%) with minor damage and/or residual displacements. Recent experimental studies [37, 27] showed that the residual drifts of posttensioned rocking columns are negligible (0.4%) compared to the pertinent drifts of conventional monolithic columns (6.8%) with the same peak drift ratios; in accordance with [32]. Further, [19, 20] showed that the stability of the rigid rocking frame is enhanced, the more heavy its cap-beam is, regardless of the rise of its center of mass; a counter-intuitive behavior.

Such self-centering systems aim to eliminate residual drifts after strong earthquakes. Many researchers [25, 26, 28, 23, 17, 43] combine the use of additional re-centering with energy dissipation devices, to propose "hybrid rocking systems" which exhibit flag-shaped hysteretic behavior (FSHB). In this context [26, 23, 17] compared numerically and experimentally the seismic performance of rocking versus conventionally designed monolithic piers. The rocking piers showed higher self-centering capacity and lower residual displacements compared to the monolithic solution. [11] examined a hybrid rocking frame with asymmetric configuration (with columns unequal in height), and compared its stability with the pertinent symmetric configuration. That study unveiled the marginal influence of the asymmetry on the stability despite the very different kinematics between the two configurations. Building on previous work on hybrid rocking structures [17, 21, 11], the present work investigates the effect of the prestressing force on the seismic performance of hybrid FSHB rocking frames, and compares different rocking design solutions.

2 ANALYTICAL MODELLING

This section examines (analytically) a rocking bridge bent which exhibits flag-shaped hysteretic behavior. The present study considers structures designed to exhibit planar rocking and it assumes no sliding between the contacting bodies takes place [5]. Consider the rocking frame of Fig. 1 enhanced with central (linear-elastic) prestressed tendons and (nonlinear-hysteretic) buckling restrained braces (BRBs) at the bottom of the piers. Note that, this study ignores the fracture of the tendons and the dissipaters, which is discussed in [11]. To describe the hysteretic behavior of the BRBs, the Bouc-Wen model [4, 42] is adopted. The restoring dissipating force is expressed as:

$$F_D = \varepsilon k_d u\left(t\right) + \left(1-\varepsilon\right) k_d u_y z\left(t\right) \tag{1}$$

where ε is the post-yield to pre-yield elastic stiffness (k_d) ratio, $u\left(t\right)$ is the axial deformation of the brace, u_y is the yield displacement equal with $u_y = 4b\sin\left(\phi_y/2\right)$ with $2b$ the width of the base of the column of the frame and ϕ_y the yield rotation (Fig. 1). $z\left(t\right)$ is a dimensionless hysteretic parameter that is governed by:

$$\dot{z}(t) = \frac{1}{u_y}\left[\dot{u}(t) - \gamma\left|\dot{u}(t)\right| z\cdot\left|z\right|^{n-1} - \beta\dot{u}(t)\left|z\right|^{n}\right] \tag{2}$$

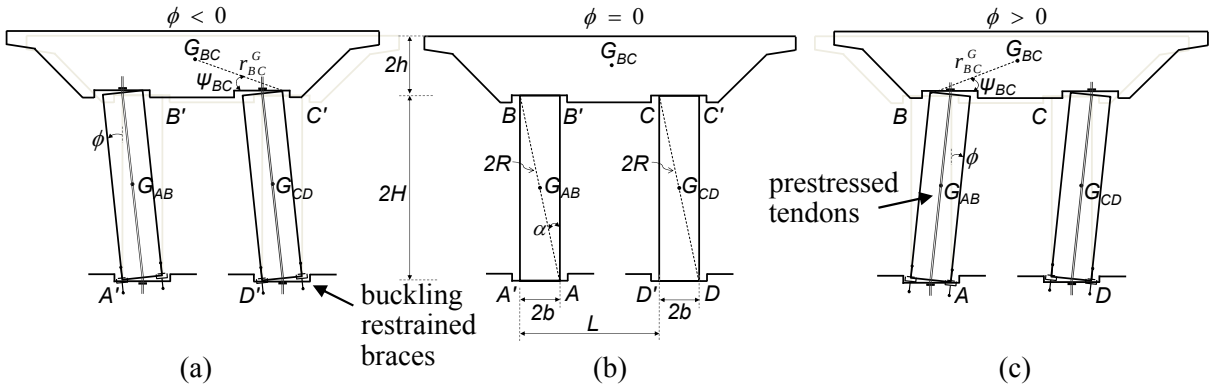

Figure 1: The examined hybrid rocking bridge bent (a) during counter-clockwise rotation, (b) at rest position and (c) during clockwise rotation.

Parameters β, γ and n control the shape of the hysteretic loop. Following [3], $\beta = 0.55$, $\gamma = 0.45$, $n = 1$, $\varepsilon = 0.025$ and $u_y = 3.5\,mm$.

2.1 Flag-shaped hysteretic behavior (FSHB)

Assuming positive (clockwise) rotations, the restoring moment offered by the weight of the two columns and the cap-beam is equal with:

$$\frac{M_R^{gr}}{2\left(m_{AB}+m_{BC}\right)gR} = \sin\left(\alpha-\phi\right) \tag{3}$$

where m_{AB} and m_{BC} are the masses of the column AB and the cap-beam BC respectively, R is the half diagonal of the column of the frame, g is the gravitational acceleration, and α is the slenderness of the column. ϕ is the generalized coordinate which describes the rocking motion of the frame (Fig. 1). The additional re-centering and energy dissipation devices offer a total restoring moment M_R^{hyb}:

$$\begin{aligned}\frac{M_R^{hyb}}{2(m_{AB}+m_{BC})gR} &= 4\left(\rho_t+\varepsilon\rho_d\right)\sin\phi + 2\sin\alpha p_{str}\cos\tfrac{\phi}{2} \\ &+8\left(1-\varepsilon\right)\rho_d\sin\tfrac{\phi_y}{2}\cos\tfrac{\phi}{2}z(t)\end{aligned} \tag{4}$$

The dimensionless parameters ρ_d, ρ_t and p_{str} control the stiffness of the dissipaters k_d, of the tendons k_t and the initial prestressing force P_0 respectively:

$$\rho_d = \frac{k_d b^2}{\left(m_{AB}+m_{BC}\right)gR},\quad \rho_t = \frac{k_t b^2}{\left(m_{AB}+m_{BC}\right)gR},\quad p_{str} = \frac{P_0}{\left(m_{AB}+m_{BC}\right)g} \tag{5}$$

The present study assumes that the design parameters ρ_d, ρ_t and p_{str} vary within $0 \le \rho_d \le 5.0$, $0 \le \rho_t \le 0.7$ and $0 \le p_{str} \le 0.1$ respectively. The total restoring moment becomes:

$$\begin{aligned}\frac{M_R}{2(m_{AB}+m_{BC})gR} &= \sin\left(\alpha-\phi\right) + 4\left(\rho_t+\varepsilon\rho_d\right)\sin\phi + 2\sin\alpha p_{str}\cos\tfrac{\phi}{2} \\ &+8\left(1-\varepsilon\right)\rho_d\sin\tfrac{\phi_y}{2}\cos\tfrac{\phi}{2}z(t)\end{aligned} \tag{6}$$

On the other hand, the overturning moment induced by the ground excitation ($\ddot{u}_g$) becomes:

$$\frac{M_{OT}}{2\left(m_{AB}+m_{BC}\right)\ddot{u}_g R} = \cos\left(\alpha-\phi\right) \tag{7}$$

Rocking initiates when the overturning moment of Eq. (7) becomes equal with the total restoring moment of Eq. (6). This equality yields the minimum ground acceleration necessary for rocking initiation:

$$\ddot{u}_{g,\min} = g \tan\alpha \, (1 + 2p_{str}) \tag{8}$$

Eq. (8) shows that increase of the prestressing force, causes increase in the ground acceleration necessary to initiate rocking. During rocking, the motion of the frame is interrupted by non-smooth impacts. At each impact, a part of the total kinetic energy is lost and the frame continues its motion with a ratio between the angular velocity after and before the impact (coefficient of restitution) equal with [11]:

$$\eta = \frac{\dot{\phi}^{+}}{\dot{\phi}^{-}} = \frac{1 - \frac{3}{2}\sin^2\alpha + 3\gamma_m \cos 2\alpha}{1 + 3\gamma_m} \tag{9}$$

The present study assumes the coefficient of restitution η to be 0.92.

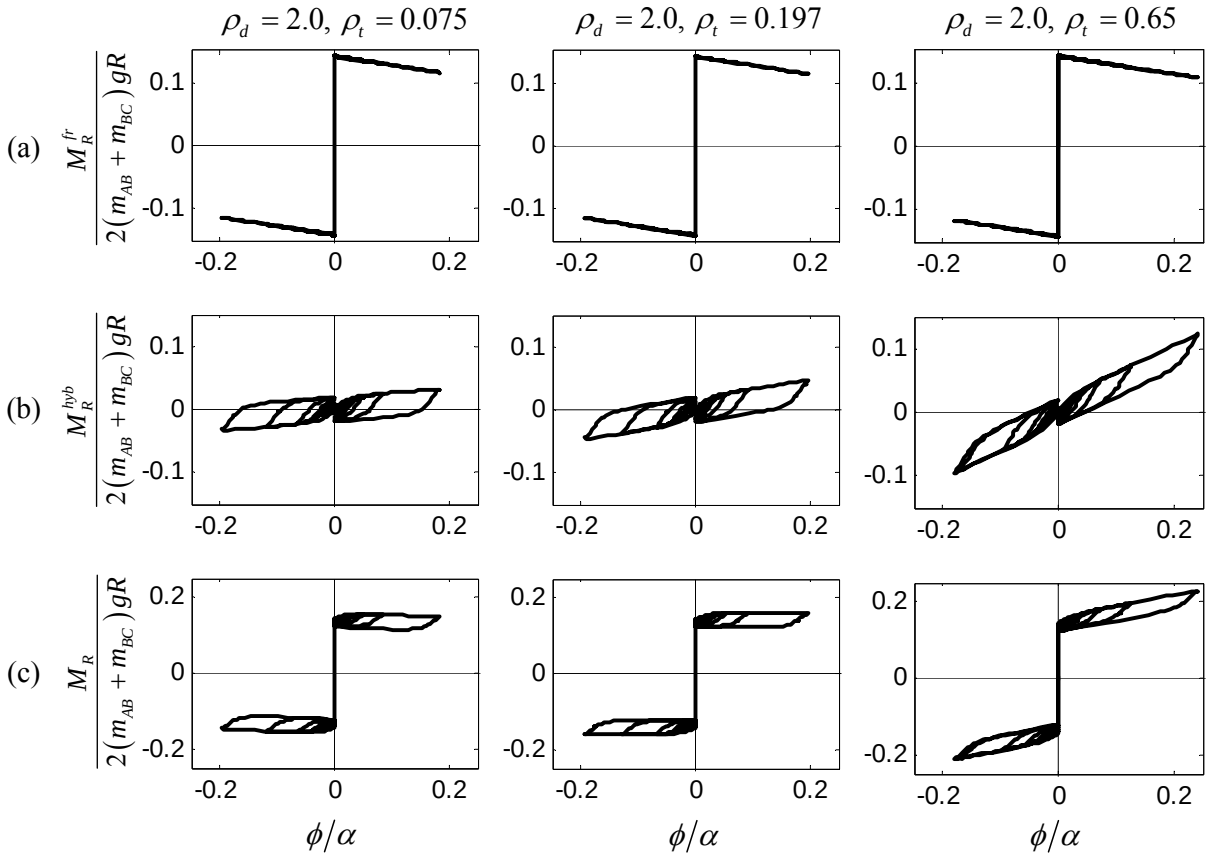

Figure 2: Restoring moments due to (a) gravitational forces, (b) the presence of tendon and dissipater and (c) total restoring moment for the rocking frame subjected to M&P pulse with $\nu_g = 45°$, $\gamma_g = 2.0$, $\alpha_g = 0.6g$ and $\omega_g = 6.09\, rad/s$.

The moment-rotation relationship follows the curves shown in Fig. 2. Observe that, the restoring moment due to the gravitational forces of the columns and the cap-beam do not enclose any area under the moment-rotation curve (Fig. 2(a)) since energy is dissipated only during impact. The presence of buckling restrained braces provides additional energy dissipation, equal with the enclosed area in Fig. 2(b). When tendons and dissipaters are combined, the hysteretic

behavior of the rocking bridge bent becomes flag-shaped (Fig. 2(c)). Note that, increase in the tendon's and the dissipater's stiffness causes increase in the overall lateral stiffness of the structure. For positive stiffness systems, it holds:

$$\rho_t + \varepsilon\rho_d > \frac{1}{4} \tag{10}$$

2.2 Equation of motion (EOM)

Fig. 1 illustrates the examined hybrid FSHB rocking frame. The equation of motion is derived using Lagrange's equation:

$$\frac{d}{dt}\left(\frac{\partial L}{\partial \dot{\phi}}\right) - \frac{\partial L}{\partial \phi} = Q \tag{11}$$

where $L = T - V$, with T the kinetic energy, V the potential energy and Q the generalized force. The kinetic energy of the system is:

$$\begin{aligned} T = I_{AB}^{pivot}\dot{\phi}^2 + m_{AB}\left[\dot{u}_g^2 + 2\dot{u}_g R\cos\left(\alpha \mp \phi\right)\dot{\phi}\right] \\ +\tfrac{1}{2}m_{BC}\left[\dot{u}_g^2 + 4R^2\dot{\phi}^2 + 4R\dot{u}_g\cos\left(\alpha \mp \phi\right)\dot{\phi}\right] \end{aligned} \tag{12}$$

where I_{AB}^{pivot} is the mass moment of inertia of the AB column with respect to the pivot point. For a rectangular column is equal with $I_{AB}^{pivot} = (4/3)\, m_{AB}R^2$. The double sign in Eq. (12) and throughout the present study denotes the sign of rotation. In particular, the upper sign corresponds to clockwise (positive) rotations and the bottom to counter-clockwise (negative) rotations.

The potential energy of the hybrid FSHB rocking frame is defined as a contribution from the gravitational and the elastic forces from the tendons. Before rocking starts, the initial prestressing force (P_0) induces an initial elongation (δl_0) to the tendon equal with $\delta l_0 = P_0/k_t$, where $k_t = EA/l$ is the elastic stiffness of the tendon with E being the Young's modulus, A the cross-sectional area and l the length of each tendon. During rocking, each tendon deforms. The elongation of each tendon is equal to the sum of the elongations at the base and the top of each tendon: $\delta l = 4b\sin\left(\phi/2\right)$. Hence, the total elongation of each tendon is $\Delta l = \delta l + \delta l_0$. Therefore, the potential energy of the hybrid FSHB rocking frame takes the form:

$$V = 2m_{AB}gR\cos\left(\alpha - \phi\right) + m_{BC}g\left[2R\cos\left(\alpha - \phi\right) + r_{BC}^{G}\sin\psi_{BC}\right] + k_t\left(4b\sin\frac{\phi}{2} + \frac{P_0}{k_t}\right)^2 \tag{13}$$

where r_{BC}^{G} is the distance from the pivot point B (or C') to the center of mass G_{BC} and the angle ψ_{BC} is shown in Fig. 1.

The calculation of the non-conservative forces Q is based on the virtual work principle $\delta W_D = Q\delta\phi$ and yields:

$$Q = -4b\cos\frac{\phi}{2}\left[\varepsilon k_d u\left(t\right) + \left(1-\varepsilon\right)k_d u_y z\left(t\right)\right] \tag{14}$$

Therefore, Eq. (11) gives:

$$\ddot{\phi} = -\frac{1+2\gamma_m}{1+3\gamma_m}p^2\left[\begin{array}{l} \sin\left(\alpha\mathrm{sgn}\left(\phi\right) - \phi\right) + \frac{\ddot{u}_g}{g}\cos\left(\alpha\mathrm{sgn}\left(\phi\right) - \phi\right) + 4\left(\rho_t + \varepsilon\rho_d\right)\sin\phi \\ +2\sin\alpha p_{str}\cos\frac{\phi}{2} + 8\left(1-\varepsilon\right)\rho_d\sin\frac{\phi_y}{2}\cos\frac{\phi}{2}z\left(t\right) \end{array}\right] \tag{15}$$

where p is the frequency parameter of the column of the frame, which for rectangular columns becomes $p = \sqrt{3g/4R}$. $\mathrm{sgn}(\phi)$ is the sign function and $\gamma_m = m_{BC}/2m_{AB}$ is the mass ratio. Ignoring the presence of the dissipater and of the prestressing force, Eq. (15) verifies the equation of motion of the symmetric rocking frame enhanced with slack (unbonded) central tendons [14], and for $\gamma_m = 0$ the pertinent equation of motion of the anchored rocking block [10].

3 SEISMIC PERFORMANCE OF THE HYBRID FSHB ROCKING BRIDGE BENT

This section examines the seismic response of the planar (freestanding and hybrid FSHB) rocking bent of Fig. 1. Consider a cap-beam 13 m wide with height $2h$ = 2 m. Assume a two-(square)-column frame with $2b$ = 1.4 m base width, same density and height $2H$ = 9.8 m each. Both columns have the same slenderness $\alpha = 8.1^\circ$ and frequency parameter $p = 1.22\ rad/s$, while the distance L is 8 m. The cap-beam/column mass ratio (γ_m) is taken as 5. The yield displacement (u_y) of the braces is assumed 3.5 mm [3], which corresponds to a yield rotation $\phi_y/\alpha = 0.018$. The present section focuses on the influence of the prestressing force on the seismic performance of the hybrid FSHB frame, while it ignores the deformation of its structural members.

3.1 Pulse-type ground motions

This study considers first pulse-type ground motions to examine the seismic performance of the hybrid FSHB rocking frame. Various mathematical expressions have been proposed in the literature that can capture the long distinct pulses of near-fault ground excitations ([41] among others). The present study adopts the Mavroeidis and Papageorgiou (M&P) [24] wavelet according to which the frequency of the pulse (ω_g), the acceleration amplitude (α_g), the number (γ_g) and the phase angle (ν_g) of half cycles are the four parameters which can idealize a wide range of near-fault ground excitations. Eq. (16) provides the expression for the ground velocity of the M&P pulse [24] with parameter A to control the velocity amplitude of the envelope of the signal.

$$\dot{u}_g(t) = \begin{cases} \frac{A}{2}\left[1+\cos\left(\frac{\omega_g}{\gamma_g}(t-t_0)\right)\right]\cos\left[\omega_p(t-t_0)+\nu_g\right], & t_0 - \frac{\pi\gamma_g}{\omega_g} \le t \le t_0 + \frac{\pi\gamma_g}{\omega_g} \\ 0 \qquad\qquad\qquad\qquad\qquad\qquad\qquad\qquad\qquad\qquad , & otherwise \end{cases} \tag{16}$$

This analysis compares the seismic performance of the freestanding and the hybrid FSHB rocking bridge bent focusing on the influence of the prestressing force. In other words, the study examines structural systems with fundamentally different behavior (i.e. negative, zero and positive post-uplift lateral stiffness) under two levels of the rocking rotation, (i) for small "safe" rotations $\phi/\alpha = 0.1$ and (ii) large "critical" rotations $\phi/\alpha = 1.0$. Recall that, $\phi/\alpha = 1.0$ represents the "critical" rotation under which the freestanding frame is considered to become unstable. In the hybrid FSHB frame the "critical" rotation increases due to the presence of the tendons and the braces. The exact "critical" rotation (ϕ_{cr}) is given by the solution of the nonlinear equation:

$$\left.\frac{\partial V_{tot}}{\partial \phi}\right|_{\phi=\phi_{cr}} = 0 \tag{17}$$

Contrary to Eq. (13), in Eq. (17) the potential energy accounts also for the presence of the braces by simplifying their behavior from nonlinear hysteretic to bilinear elastic. Thus, the total

potential energy of the system becomes [15]:

$$V_{tot} = 2m_{AB}gR\cos(\alpha-\phi) + m_{BC}g\left[2R\cos(\alpha-\phi) + r_{BC}^{G}\sin\psi_{BC}\right] \\ +k_t\left(4b\sin\tfrac{\phi}{2} + \tfrac{P_0}{k_t}\right)^2 + 16(1-\varepsilon)k_d b^2\sin\tfrac{\phi_y}{2}\sin\tfrac{\phi}{2} + 8\varepsilon k_d b^2\sin^2\tfrac{\phi}{2} \tag{18}$$

Therefore, Eq. (17) gives:

$$\sin(\alpha-\phi_{cr}) + 4\rho_t\sin\phi_{cr} + 2\varepsilon\rho_d\sin\phi_{cr} + 4(1-\varepsilon)\rho_d\sin\frac{\phi_y}{2}\cos\frac{\phi_{cr}}{2} + \frac{2b}{R}p_{str}\cos\frac{\phi_{cr}}{2} = 0 \tag{19}$$

Eq. (19) provides the "critical" rotation of hybrid FSHB rocking bridge bents for various values of the (dimensionless) design parameters ρ_d, ρ_t and p_{str}. The combination of the design parameters ρ_t and ρ_d, yield structural systems with (i) tendons flexible enough, such that the frame maintains its negative stiffness, (ii) zero overall stiffness and (iii) stiffer tendons so that the rocking frame exhibits positive post-uplift lateral stiffness. Recall that, the fracture of the tendons and braces is ignored, hence hybrid rocking frames with zero or positive lateral stiffness theoretically will not overturn.

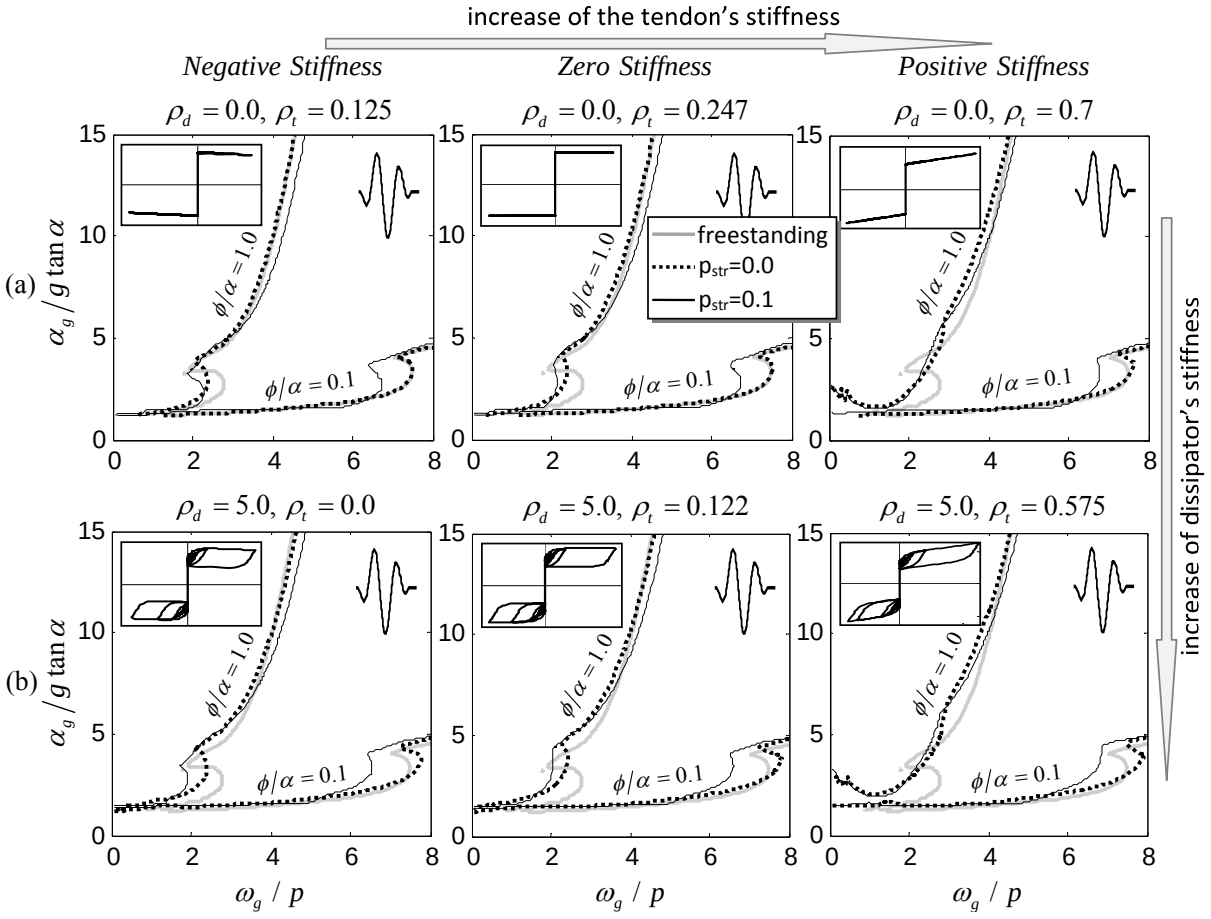

Figure 3: Seismic performance of the rocking bridge bent subjected to M&P pulse with $\nu_g = 45°$, $\gamma_g = 2.0$ for different levels of prestress and for the following dissipation parameters (a) $\rho_d = 0.0$ and (b) $\rho_d = 5.0$.

Fig. 3 compares rocking frames with negative, zero and positive post-uplift lateral stiffness under pulse-type ground motions. Fig. 3 unveils the diverse role of the prestressing force on

the seismic performance of the hybrid FSHB rocking frame. In particular, for large rocking rotations ($\phi/\alpha = 1.0$) and as the size of the columns increases ($\omega_g/p > 3$), the prestressing force has negative effect on the stability of the frame; the lower the prestress the higher the seismic stability. This is true regardless of the sign of the lateral stiffness, but more pronounced to negative stiffness systems. Overall for large rocking rotations, both the freestanding and the hybrid with zero prestressing force exhibit the highest seismic rotation. On the contrary, for either small-sized rocking columns ($\omega_g/p < 3$) and large rotations ($\phi/\alpha = 1.0$) or large rocking columns ($\omega_g/p > 6$) and small rotations ($\phi/\alpha = 0.1$), the prestressing force has beneficial influence on the performance.

Further, note that each column of Fig. 3 considers frames with the same (negative, zero, or positive) lateral stiffness. The ρ_d increase effect is slightly favorable regardless of the sign of the overall stiffness. In addition, increasing the stiffness of the tendons (i.e. increasing ρ_t), the overall lateral stiffness of the system increases. However, Fig. 3 shows that this increase doesn't lead to superior seismic performance (e.g. Fig. 3(a)).

3.2 Historic excitations

The present section examines the seismic response of the hybrid FSHB rocking frame to historic ground motions, regardless of whether they contain distinguishable pulses or not. It employs a well-known set of historic ground motions scaled to yield a probability of exceedance of 2% in 50 years [31].

Number	Record	Magnitude	Scale factor	dt(s)	Duration(s)	PGA(cm/s^2)
SE21	1992 Mendocino	7.1	0.98	0.02	59.98	741.13
SE22	1992 Mendocino	7.1	0.98	0.02	59.98	476.22
SE23	1992 Erzincan	6.7	1.27	0.005	20.775	593.60
SE24	1992 Erzincan	6.7	1.27	0.005	20.775	529.06
SE25	1949 Olympia	6.5	4.35	0.02	79.98	878.23
SE26	1949 Olympia	6.5	4.35	0.02	79.98	805.68
SE27	1965 Seattle	7.1	10.04	0.02	81.82	1722.40
SE28	1965 Seattle	7.1	10.04	0.02	81.82	1364.70
SE29	1985 Valpariso	8.0	2.9	0.025	99.975	1605.50
SE30	1985 Valpariso	8.0	2.9	0.025	99.975	1543.50
SE31	1985 Valpariso	8.0	3.96	0.025	99.975	1246.20
SE32	1985 Valpariso	8.0	3.96	0.025	99.975	884.43
SE35	1978 Miyagi-oki	7.4	1.78	0.02	79.98	595.07
SE36	1978 Miyagi-oki	7.4	1.78	0.02	79.98	768.62

Table 1: Earthquake records with probability of exceedance of 2% in 50 years (adapted from [31].

Figs 4, 5 compare the response of the examined rocking frames in terms of peak rotation and time history analysis respectively. Both Figs 4, 5 verify the high seismic performance of the examined rocking frames, since all of them survive the excitations even though the earthquake records are scaled to the maximum credible earthquake level. Note that, according to the assumptions of the present analysis, when the structure survives the excitation, it eventually re-centers with no permanent displacement and/or expected damage. In particular, Fig. 4 confirms the influence of the prestressing force on the seismic behavior. Prestressing the tendons

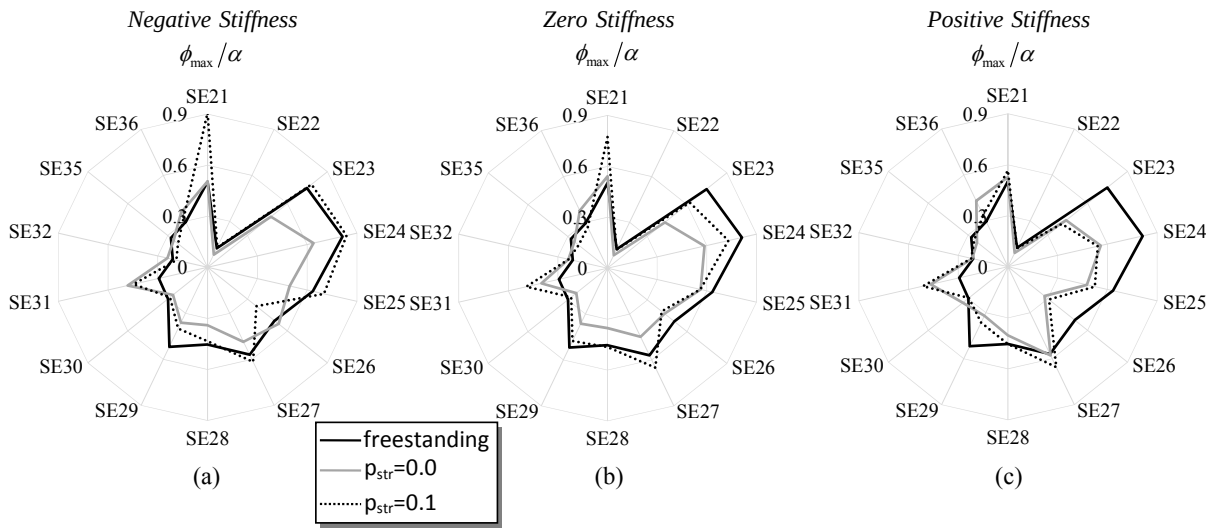

Figure 4: Maximum rotations for the freestanding and hybrid FSHB rocking bridge bent with (a) negative ($\rho_t = 0.075$), (b) zero ($\rho_t = 0.197$), (c) positive ($\rho_t = 0.65$) stiffness, $\rho_d = 2.0$ and different levels of prestress.

deteriorates the seismic performance of the hybrid FSHB rocking frame regardless of the sign of the overall stiffness. This degrading effect becomes even more pronounced on negative stiffness systems when the frame sustains large rocking rotations (see for instance $SE21$, $SE23$, $SE24$ $SE25$, $SE27$ in Figs 4(a), 5). In that cases, both the freestanding and the hybrid frame with slack tendons ($p_{str} = 0$) outperform the hybrid FSHB with $p_{str} = 0.1$. On the contrary, when the frame undergoes small rotations, the prestressing force has indeed beneficial effect (e.g. $SE30$, $SE32$, $SE35$, $SE36$ in Figs 4(a), 5).

Further, Fig. 4 shows that increase of the stiffness of the structure (i.e. from negative to positive) has beneficial effect on the seismic performance of the hybrid FSHB without however changing the effect of the prestress, which remains detrimental regardless of the sign of the lateral stiffness. This (slight) enhancement though, comes at the cost of higher energy demands by the buckling restrained braces (as Fig. 6 shows). Specifically, Fig. 6 compares hybrid FSHB rocking frames with negative, zero and positive overall lateral stiffness, in terms of the net dissipated hysteretic energy. Fig. 6 shows that negative stiffness systems yield the lowest energy demands. This is attributed to the fact that a negative stiffness system cannot resonate (in a classical sense). Overall, positive stiffness systems exhibit the highest energy needs. In other words, the rocking rotation mitigation due to the increased stiffness, comes at the cost of higher energy demands by the dissipaters. Fig. 6 shows that increase of the prestress does not lead to higher energy demands, since for most records the energy dissipated by the braces is slightly lower for prestressed hybrid FSHB frames ($p_{str} \neq 0$) than for slack hybrid FSHB frames ($p_{str} = 0$).

In summary Figs. 3, 4, 5 and 6 show that depending on the characteristics of the examined earthquake record, a different rocking design solution (i.e. freestanding or hybrid with negative, zero, or positive post-uplift lateral stiffness) might yield the optimal rocking design solution in terms of seismic performance. Therefore, the assessment of the seismic performance of hybrid FSHB rocking bridge bents beckons for a probabilistic evaluation [12], which is not however the scope of the present study.

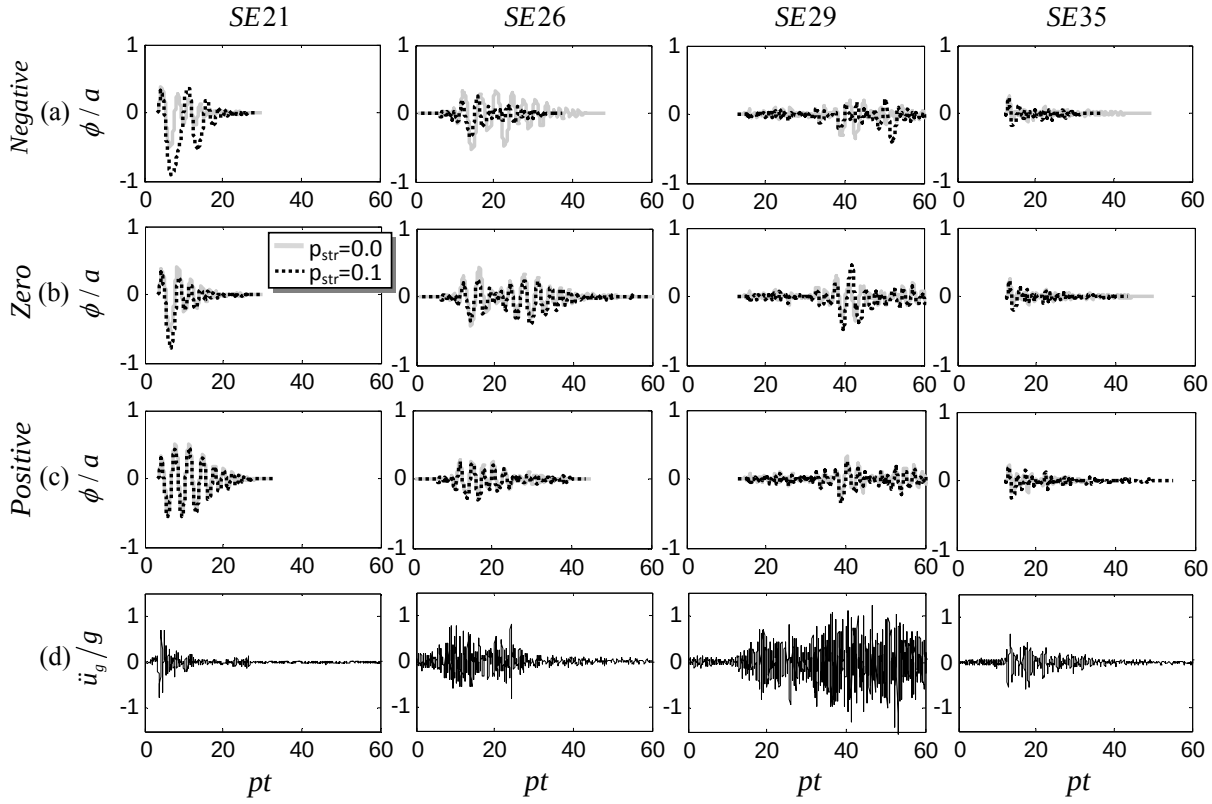

Figure 5: Time history analysis for the hybrid FSHB rocking bridge bent with (a) negative ($\rho_t = 0.075$), (b) zero ($\rho_t = 0.197$), (c) positive ($\rho_t = 0.65$) stiffness, $\rho_d = 2.0$ and different levels of prestress.

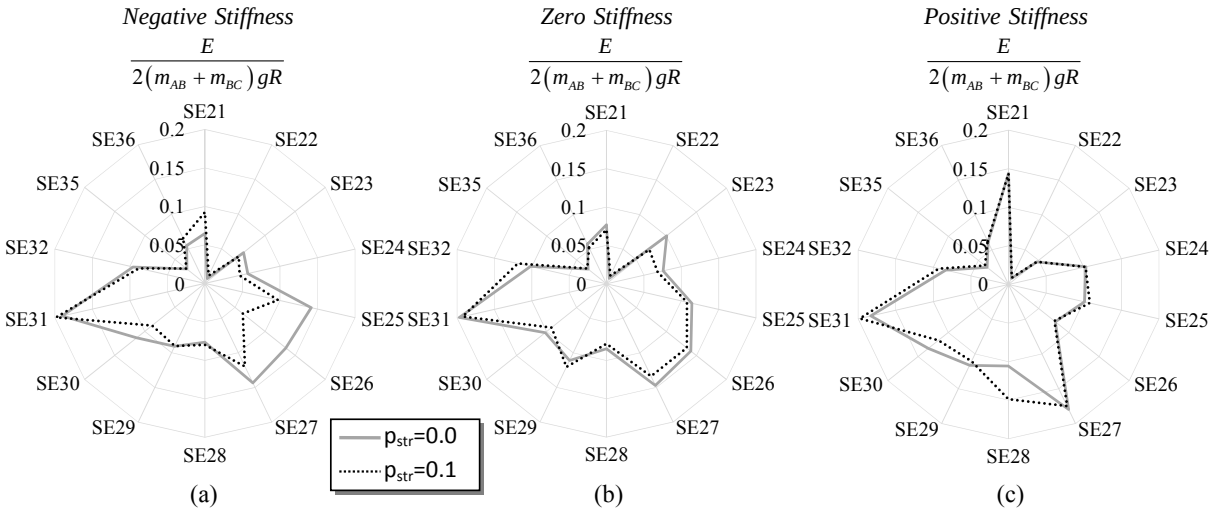

Figure 6: Net dissipated energy for the hybrid FSHB rocking bridge bent with (a) negative ($\rho_t = 0.075$), (b) zero ($\rho_t = 0.197$), (c) positive ($\rho_t = 0.65$) stiffness $\rho_d = 2.0$ and different levels of prestress.

4 CONCLUSIONS

This study investigates the seismic performance of planar freestanding and hybrid rocking frames with flag-shaped hysteretic behavior. This work demonstrates the diverse role of the prestressing force on the performance of the hybrid FSHB rocking bents. Prestressing the tendons deteriorates the frame's seismic performance when it sustains large rocking rotations and as the size of the columns increases; a counter-intuitive conclusion. On the contrary, either for small-sized rocking columns and large rocking rotations or for large-sized rocking columns and small rocking rotations, the influence of the prestress becomes beneficial in restoring the frame. The analysis also confirms the beneficial influence of the dissipater, which is more pronounced for negative stiffness rocking frames. Increasing the overall stiffness, the seismic performance of the frame is slightly enhanced at the expense, however, of higher energy demands by the dissipaters. This is not the case for the prestressing force, since increasing the prestress does not lead to higher energy demands. Finally, this work confirms the sensitivity of the examined rocking frames (freestanding and hybrid FSHB) to the characteristics of the adopted earthquake records, and that none of the rocking design solutions examined is optimal in all cases.

5 ACKNOWLEDGMENTS

Financial support was provided by the Research Grants Council of Hong Kong, under grant reference number ECS 639613.

REFERENCES

[1] Acikgoz, S., DeJong, M. J., The interaction of elasticity and rocking in flexible structures allowed to uplift. *Earthquake Engineering & Structural Dynamics*, **41**(15), 2177–2194, 2012.

[2] Acikgoz, S., DeJong, M. J., The rocking response of large flexible structures to earthquakes. *Bulletin of earthquake engineering*, **12**(2), 875–908, 2014.

[3] Black, C. J., Makris, N., Aiken, I. D., Component testing, seismic evaluation and characterization of buckling-restrained braces. *Journal of Structural Engineering*, **130**(6), 880–894, 2004.

[4] Bouc, R., Forced vibration of mechanical systems with hysteresis. *Proceedings of the fourth conference on non-linear oscillation*, Prague, Czechoslovakia, 1967.

[5] Brogliato, B., Zhang, H., Liu, C., Analysis of a generalized kinematic impact law for multibody-multicontact systems, with application to the planar rocking block and chains of balls. *Multibody System Dynamics*, **27**(3), 351–382, 2012.

[6] Chen, Y. H., Liao, W. H., Lee, C. L., Wang, Y. P., Seismic isolation of viaduct piers by means of a rocking mechanism. *Earthquake engineering & structural dynamics*, **35**(6), 713–736, 2006.

[7] Cheng, C. T., Shaking table tests of a self-centering designed bridge substructure. *Engineering Structures*, **30**(12), 3426–3433, 2008.

[8] DeJong, M. J., Dimitrakopoulos, E. G., Dynamically equivalent rocking structures. *Earthquake Engineering & Structural Dynamics*, **43**(10), 1543–1563, 2014.

[9] Dimitrakopoulos, E. G., DeJong, M. J., Revisiting the rocking block: closed-form solutions and similarity laws. *Proceedings of the Royal Society A: Mathematical, Physical and Engineering Science*, **468**(2144), 2294–2318, 2012.

[10] Dimitrakopoulos, E. G., DeJong, M. J., Overturning of retrofitted rocking structures under pulse-type excitations. *Journal of Engineering Mechanics*, **138**(8), 963–972, 2012.

[11] Dimitrakopoulos, E. G., Giouvanidis, A. I., Seismic response analysis of the planar rocking frame. *Journal of Engineering Mechanics*, **141**(7), 04015003, 2015.

[12] Dimitrakopoulos, E. G., Paraskeva, T. S., Dimensionless fragility curves for rocking response to near-fault excitations. *Earthquake Engineering & Structural Dynamics*, **44**(12), 2015-2033, 2015.

[13] ElGawady, M. A., Ma, Q., Butterworth, J. W., Ingham, J., Effects of interface material on the performance of free rocking blocks. *Earthquake Engineering & Structural Dynamics*, **40**(4), 375–392, 2011.

[14] Giouvanidis, A. I., Dimitrakopoulos, E. G., Seismic analysis of hybrid rocking bridge bents. *Second European Conference on Earthquake Engineering and Seismology*, Istanbul, Turkey, 2014.

[15] Giouvanidis, A. I., Dimitrakopoulos, E. G., Seismic performance of rocking frames with flag-shaped hysteretic behavior. *Journal of Engineering Mechanics*, **under review**, 2016.

[16] Housner, G. W., The behavior of inverted pendulum structures during earthquakes. *Bulletin of the seismological society of America*, **53**(2), 403–417, 1963.

[17] Kam, W. Y., Pampanin, S., Palermo, A., Carr, A. J., Self-centering structural systems with combination of hysteretic and viscous energy dissipations. *Earthquake Engineering & Structural Dynamics*, **39**(10), 1083–1108, 2010.

[18] Kirkpatrick, P., Seismic measurements by the overthrow of columns. *Bulletin of the Seismological Society of America*, **17**(2), 95–109, 1927.

[19] Makris, N., Vassiliou, M. F., Planar rocking response and stability analysis of an array of free-standing columns capped with a freely supported rigid beam. *Earthquake Engineering & Structural Dynamics*, **42**(3), 431–449, 2012.

[20] Makris, N., Vassiliou, M. F., Are Some Top-Heavy Structures More Stable?. *Journal of Structural Engineering*, **140**(5), 06014001, 2014.

[21] Makris, N., Vassiliou, M. F., Dynamics of the rocking frame with vertical restrainers. *Journal of Structural Engineering*, **141**(10), 04014245, 2014.

[22] Mander, J. B., Cheng, C.-T., *Seismic resistance of bridge piers based on damage avoidance design, Report No. NCEER-97-0014*, University at Buffalo, 1997.

[23] Marriott, D., Pampanin, S., Palermo, A., Quasi-static and pseudo-dynamic testing of unbonded post-tensioned rocking bridge piers with external replaceable dissipaters. *Earthquake Engineering & Structural Dynamics*, **38**(3), 331–354, 2009.

[24] Mavroeidis, G. P., Papageorgiou, A. S., A mathematical representation of near-fault ground motions. *Bulletin of the Seismological Society of America*, **93**(3), 1099–1131, 2003.

[25] Palermo, A., Pampanin, S., Calvi, G. M., Concept and development of hybrid solutions for seismic resistant bridge systems. *Journal of Earthquake Engineering*, **9**(6), 899–921, 2005.

[26] Palermo, A., Pampanin, S., Marriott, D., Design, modeling, and experimental response of seismic resistant bridge piers with posttensioned dissipating connections. *Journal of Structural Engineering*, **133**(11), 1648–1661, 2007.

[27] Panagiotou, M., Trono, W., Jen, G., Kumar, P., Ostertag, C. P., Experimental seismic response of hybrid fiber-reinforced concrete bridge columns with novel longitudinal reinforcement detailing. *Journal of Bridge Engineering*, **20**(7), 04014090, 2014.

[28] Pollino, M., Bruneau, M., Seismic retrofit of bridge steel truss piers using a controlled rocking approach. *Journal of Bridge Engineering*, **12**(5), 600–610, 2007.

[29] Psycharis, I. N., Jennings, P. C., Rocking of slender rigid bodies allowed to uplift. *Earthquake Engineering & Structural Dynamics*, **11**(1), 57–76, 1983.

[30] Psycharis, I. N., Fragiadakis, M., Stefanou, I., Seismic reliability assessment of classical columns subjected to near-fault ground motions. *Earthquake Engineering & Structural Dynamics*, **42**(14), 2061–2079, 2013.

[31] S.A.C., *Suites of earthquake ground motions, Structural Engineers Association of California (SEA), Applied Technology Council (ATC) and Consortium of Universities for Research in Earthquake Engineering (CUREE)*, <http://nisee.berkeley.edu> 1997.

[32] Sakai, J., Mahin, S. A., Mitigation of residual displacements of circular reinforced concrete bridge columns. *13th World Conference on Earthquake Engineering Proceedings*, Vancouver, Canada, 2004.

[33] Schaefer, J. A., Kennedy, B., Eberhard, M. O., Stanton, J. F., *Unbonded pretensioned bridge columns with rocking detail, Report No. PEER 2014/08*, University of Washington, 2014.

[34] Sritharan, S., Aaleti, S., Henry, R. S., Liu, K. Y., Tsai, K. C., Precast concrete wall with end columns (PreWEC) for earthquake resistant design. *Earthquake Engineering & Structural Dynamics*, **44**(12), 2075–2092, 2015.

[35] Stathas, N., Skafida, S., Bousias, S. N., Fardis, M. N., Digenis, S., Palios, X., Hybrid simulation of bridge pier uplifting. *Bulletin of Earthquake Engineering*, **DOI:10.1007/s10518-015-9822-2**, 1–14, 2015.

[36] Thonstad, T., Mantawy, I. M., Stanton, J. F., Eberhard, M. O., Sanders, D. H., Shaking Table Performance of a New Bridge System with Pretensioned Rocking Columns. *Journal of Bridge Engineering*, **21**(4), 04015079, 2016.

[37] Trono, W., Jen, G., Panagiotou, M., Schoettler, M., Ostertag, C. P., Seismic response of a damage-resistant recentering posttensioned-hyfrc bridge column. *Journal of Bridge Engineering*, **20**(7), 04014096, 2014.

[38] Truniger, R., Vassiliou, M. F., Stojadinovic B., An analytical model of a deformable cantilever structure rocking on a rigid surface: experimental validation. *Earthquake Engineering & Structural Dynamics*, **44**(15), 2795–2815, 2015.

[39] Vassiliou, M. F., Mackie, K. R., Stojadinovic B., Dynamic response analysis of solitary flexible rocking bodies: modeling and behavior under pulse-like ground excitation. *Earthquake Engineering & Structural Dynamics*, **43**(10), 1463–1481, 2014.

[40] Vassiliou, M. F., Truniger, R., Stojadinovic B., An analytical model of a deformable cantilever structure rocking on a rigid surface: development and verification. *Earthquake Engineering & Structural Dynamics*, **44**(15), 2775–2794, 2015.

[41] Voyagaki, E., Mylonakis, G., Psycharis, I. N., Rigid block sliding to idealized acceleration pulses. *Journal of Engineering Mechanics*, **138**(9), 1071–1083, 2012.

[42] Wen, Y.-K., Method for random vibration of hysteretic systems. *Journal of the engineering mechanics division*, **102**(2), 249–263, 1976.

[43] White, S., Palermo, A., Quasi-Static Testing of Posttensioned Nonemulative Column-Footing Connections for Bridge Piers. *Journal of Bridge Engineering*, **DOI:10.1061/(ASCE)BE.1943-5592.0000872**, 04016025, 2016.